A&A 657, A105 (2022)
https://doi.org/10.1051/0004-6361/202142173

Astronomy & Astrophysics

Highly sensitive search for magnetic fields in white dwarfs using broad-band circular polarimetry

Andrei V. Berdyugin[1], Vilppu Piirola[1], Stefano Bagnulo[2], John D. Landstreet[2,3], and Svetlana V. Berdyugina[4]

[1] Department of Physics and Astronomy, University of Turku, 20014 Turku, Finland
e-mail: andber@utu.fi, piirola@utu.fi
[2] Armagh Observatory and Planetarium, College Hill, Armagh BT61 9DH, UK
e-mail: stefano.bagnulo@armagh.ac.uk
[3] Department of Physics & Astronomy, University of Western Ontario, London, Ontario N6A 3K7, Canada
[4] Leibniz-Institut für Sonnenphysik (KIS), Schöneckstr 6, Freibirg, Germany

Received 8 September 2021 / Accepted 28 October 2021

ABSTRACT

Circular polarisation measurements of white dwarfs of various ages and spectral types are useful to understand the origin and evolution of the magnetic field in degenerate stars. In the latest stages of white dwarf evolution, when stars are so cool that spectral lines are no longer formed in the normal H- or He-dominated atmospheres, magnetic fields can be probed only by means of circular polarimetry of the continuum. The study of the fields of featureless DC white dwarfs may reveal whether Ohmic decay acts on magnetic white dwarfs, or if magnetic fields continue to be generated even several billion years after white dwarf formation. Compared to spectropolarimetry, broad-band circular polarisation measurements have the advantage of reaching a higher accuracy in the continuum, with the potential of detecting magnetic fields as weak as a fraction of a MG in DC stars, if the telescope size is adequate for the star's magnitude. Here we present the results of a first (short) observing campaign with the DIPol-UF polarimeter, which we have used to measure broad-band circular polarisation of white dwarfs. Our observing run was in part aimed to fully characterise the instrument, and in part to study the relationship between magnetic field strength (when known from spectropolarimetry) and circular polarisation of the continuum. We also observed a small number of previously unexplored DC white dwarfs, and we present the discovery of two new magnetic white dwarfs of spectral class DC, probably the first discovery of this kind made with broad-band circular polarimetric techniques since the late 1970s. We also discuss the characteristics of our instrument, and predict the level of polarimetric accuracy that may be reached as a function of stellar magnitude, exposure time, and telescope size.

Key words. white dwarfs – stars: magnetic field – polarization

1. Introduction

White dwarfs (WDs) are the end point of 90% of stellar evolution. About 20% of such stars possess strong magnetic fields, but if we exclude stars younger than 0.5 Gyr from the statistics, this frequency rises to almost 30% (Bagnulo & Landstreet 2021). The distribution of the field strength is approximately uniform per decade, in a range that varies from a few tens of KG to several hundred MG, and there are no obvious signs of Ohmic decay during WD cooling, at least until an age of 5 Gyr (Landstreet & Bagnulo 2019; Bagnulo & Landstreet 2021). The origin of these fields is not fully understood. Several hypotheses have been put forward: for instance, a field could be inherited from pre-WD evolution, or originate during the merging of a binary system, or it might be produced by a dynamo acting after crystallisation begins (Isern et al. 2017). None of the proposed mechanisms is able to explain all observed magnetic features of degenerate stars, and more than one channel of field formation may exist.

Magnetic fields are primarily detected through the analysis of the Zeeman effect on the Stokes profiles of spectral lines produced in the atmospheres of almost pure H or He found in most WDs. Zeeman splitting may be detected with high-resolution spectroscopy in DA, DB, and DZ WDs (with prominent H, He, and sometimes Ca or Fe lines) that have field strengths as low as 50 kG. More commonly, from low-resolution spectroscopy, the usual detection limit is of the order of 1 MG. With spectropolarimetry, the detection threshold is 1−3 dex lower. Circular polarimetry is sensitive to the component of the magnetic field along the line of sight averaged over the stellar disk. For this quantity, usually called mean longitudinal field ($\langle B_z \rangle$), values as small as a few kG may be detected in DA and DB stars (Aznar Cuadrado et al. 2004; Landstreet & Bagnulo 2019).

The situation is different in featureless (DC) stars, in which a magnetic field may be detected only if its strength is sufficiently high to circularly polarise the continuum. Assuming that a 15 MG field is needed to produce 1% of polarisation (Bagnulo & Landstreet 2020), the weakest fields detected so far in DC WDs are of the order of several MG. However, it is in principle possible to firmly detect circular polarisation signals of the order of a few parts in 10^{-4}, or even smaller, and thus to detect magnetic fields in DC WDs as weak as a fraction of a MG (if such fields exist in DC stars). Bagnulo & Landstreet (2021) have suggested that the field strength may be roughly uniformly distributed per decade in a range between a few tens of kG and few hundred MG. Recalling that the magnetic frequency in older stars is of the order of 30%, we conclude that with appropriate exposure time and telescope size, and with an instrument capable of delivering a polarimetric sensitivity of order 10^{-4}, one would expect to detect a magnetic field in at least one out of five DC WDs.

Estimating the frequency of magnetic fields in DC WDs as a function of stellar age would be very useful to establish whether Ohmic decay operates during DC WD cooling, and if so, on which timescale; whether the field strength starts to decrease with time after a certain age; and if there is an age at which none of the DC stars are found to be magnetic. These data would help to set strong constraints to the theories that try to explain the origin and evolution of magnetic fields in degenerate stars.

The circular polarisation of the continuum may be measured with a photo-multiplier tube (PMT) or in imaging mode with a CCD detector, through narrow- or broad-band filters, or even in white light without any filter at all; or with spectropolarimetric techniques. Narrow- and broad-band circular polarisation (BBCP) measurements were extensively used in the 1970s (e.g. Kemp et al. 1970; Angel & Landstreet 1970a; Landstreet & Angel 1971) and the early 1980s (Liebert & Stockman 1980; Angel et al. 1981), but have never been systematically exploited during the past four decades. However, spectropolarimetry of the continuum for surveys of DC WDs has been used by Putney (1997), and more recently, by Bagnulo & Landstreet (2020, 2021) for a systematic survey of DC WDs of the local 20 pc volume.

Spectropolarimetry potentially has a much higher diagnostic content than BBCP because the detailed behaviour of the polarised spectrum with wavelength is dictated by the field strength, atmospheric chemistry, and morphology. Spectral resolution may be traded with the signal-to-noise ratio, S/N, via software, allowing one in principle to reach the same S/N as in BBCP after heavy re-binning, if this is necessary with faint stars. However, Bagnulo & Landstreet (2020, 2021) have argued that the spectropolarimetry of the continuum is generally affected by higher instrumental and background polarisation than BBCP, making it effectively very difficult to assess the reliability of any signal smaller than 10^{-3}, no matter how high the S/N is. BBCP techniques have been proved to reach a sensitivity better than 10^{-4} and should therefore be regarded as the technique of choice for the detection of the weakest fields in DCs stars, but also for larger surveys, to be followed up by spectropolarimetric monitoring once a magnetic WD has been identified.

We have developed high-precision polarimeters for applications of broad-band linear polarimetry, ranging from studies of the minute polarisation produced by interstellar dust and the magnetic field in the solar neighbourhood to strongly interacting binary stars with a BH component. Our Dipol-2 polarimeter (Piirola et al. 2014) and the more recent version, DIPol-UF (Piirola et al. 2021), achieve precision at the 10^{-5} level. We expect to reach a similar performance level in circular polarimetry for sufficiently bright stars. With this in mind, we initiated a pilot study to explore the capabilities of the instrument in circular polarimetry of magnetic WDs, and the prospects for applying the BBCP techniques in general. In this paper we discuss the results of our study, and report new discoveries of previously unknown magnetic WDs.

2. Observations and data reduction

2.1. Instrument description

The observations were carried out at the 2.5 m Nordic Optical Telescope (NOT, located at the Observatorio del Roque de los Muchachos, La Palma, Canary Islands) on three nights, 2021 July 2–5, using the simultaneous three-colour ($B'V'R'$) polarimeter DIPol-UF. The polarimeter is described in detail by Piirola et al. (2021).

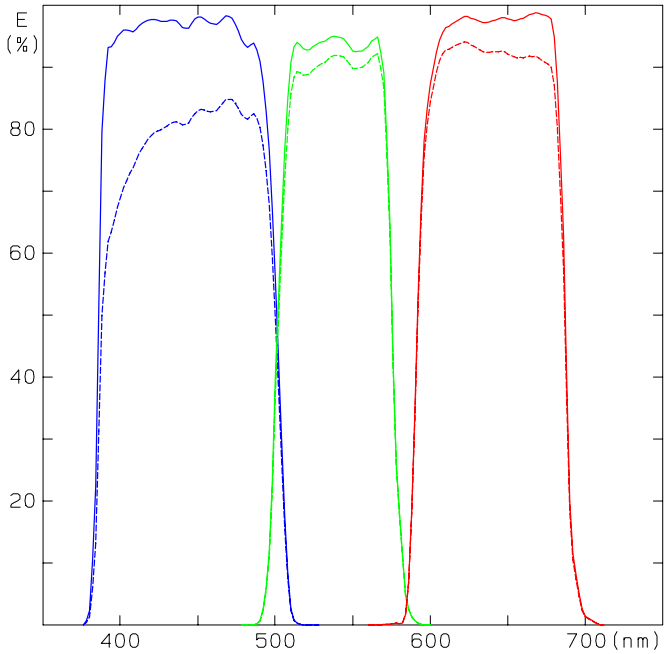

Fig. 1. DIPol-UF passbands ($B'V'R'$) determined by the filters and dichroic beam splitters, in the blue (B'), green (V'), and red (R') spectral region (continuous lines). Dashed lines show the effect of the quantum efficiency of the CCD detectors taken into account.

The light enters DIPol-UF through the modulator, a B. Halle superachromatic quarter-wave plate (QWP) for circular polarisation measurements. The plate is rotated to discrete positions with steps of 90° for circular polarimetry, and it remains at a fixed angle while each exposure is in progress. The optical axis of the QWP is at 45° from the polarisation planes of the analyser. A plane-parallel calcite plate acts as a polarisation analyser and splits the incident radiation into two orthogonally linearly polarised rays (ordinary and extraordinary). With the image scale of the NOT, the o- and e-image separation is about 14.6″. Two dichroic beam splitters split the light into the three ($B'V'R'$) spectral passbands, with equivalent wavelengths of 445, 540, and 640 nm, and a full width at half maximum, FWHM, of 114, 75, and 96 nm, respectively (Fig. 1). We emphasise that our $B'V'R'$ bands are not those of the Johnson-Cousins system, since broad overlapping passbands cannot be created by the dichroic beam splitters. Instead, we use sharp-cutoff filters with high peak transmission. The V' band is somewhat narrower than the other bands due to the particular filter used for that band in addition to the dichroic beam splitters.

DIPol-UF uses three ultrafast electron-multiplied (EM) Andor iXon CCD cameras. The V' and R' cameras are identical iXon Ultra 897-EX models, while for the B' passband, the iXon Ultra 897-BV model with the sensitivity optimised for the blue region is used. Faint targets are recorded in the EM amplifier mode with the EM gain value in the range of 5−20. In the EM mode, the camera can achieve single-photon sensitivity owing to the elimination of the readout noise, which significantly increases the S/N. For bright targets, conventional amplifiers with higher dynamical range are used in combination with a defocusing technique. The minimum number of the optical elements, high throughput, negligible systematic effects, and direct optical elimination of sky polarisation make DiPol-UF a very efficient instrument for broad-band polarimetry. The sensitivity of DIPol-UF in measuring polarisation is limited in practice by

Table 1. Programme stars and their main physical features.

Star		G	d (pc)	$T_{\rm eff}$ (K)	log g c.g.s.	M ($M_\odot$)	Age (Gyr)	Previous observations
WD 1309+853	G 256–7	15.8	16.5	5300	8.12	0.66	5.46	DA MWD with $\langle\|B\|\rangle \simeq 5.4$ MG (7)
WD 1350−090	GJ 3814	14.6	19.7	9580	8.13	0.68	0.81	DA MWD with $\langle\|B\|\rangle \simeq 0.45$ MG (5,15)
WD 1503−070	GD 175	15.8	20.3	6640	8.00	0.59	1.80	DA MWD with $\langle B_z\rangle \sim 2$ MG (12)
WD 1556+044	PM J15589+0417	16.0	22.5	6685	8.43	0.85	3.65	DC (He) never observed
WD 1647+591	DN Dra	12.3	10.9	12 738	8.24	0.76	0.45	Non magnetic DA WD (13)
WD 1748+708	G 240–72	13.8	6.2	5570	8.34	0.79	5.86	Known strongly polarised DQ WD (2,4,9)
WD 1831+197	G 184–12	16.3	39.3	7305	8.04	0.60	1.57	DQ (He) no polarisation detected (8)
WD 1856+534	LP 141–14	17.0	24.8	4430	7.69	0.40	4.34	DC (He) never observed
WD 1900+705	Grw +70° 8247	13.3	12.9	11 880	8.54	0.93	0.92	Known strongly polarised DA WD (1)
WD 1953−011	LAWD 79	13.6	11.6	7868	8.23	0.73	1.63	DA6 MWD ($\langle B_z\rangle \sim 0.1$ MG with spot) (6,10)
WD 2011+063	G 24–9	15.7	22.9	6455	8.10	0.63	2.34	DC (He) no polarisation detected (3,8)
WD 2032+248	HD 340611	11.6	14.8	20 704	8.03	0.64	0.06	Non magnetic DA WD (13)
WD 2049−253	UCAC4 325–215293	16.0	18.0	4895	7.84	0.48	4.4	DC MWD (14)
WD 2049−222	LP 872–48	15.0	20.3	8164	8.33	0.79	1.97	DC (He) never observed
WD 2117+539	EGGR 378	12.4	17.3	15 250	7.94	0.58	0.17	Non magnetic DA WD (13)
WD 2254+076	G 28–27	17.1	45.5	12 847	9.26	1.29	~1.8	DA MWD with $\langle\|B\|\rangle \simeq 16$ MG (11)

References. Key to references: 1: Kemp et al. (1970); 2: Angel et al. (1974); 3: Angel et al. (1981); 4: West (1989); 5: Schmidt & Smith (1994); 6: Schmidt & Smith (1995); 7: Putney (1995); 8: Putney (1997); 9: Berdyugin & Piirola (1999); 10: Valyavin et al. (2008); 11: Külebi et al. (2009); 12: Gianninas et al. (2011); 13: Bagnulo & Landstreet (2018); 14: Bagnulo & Landstreet (2020); 15: Bagnulo & Landstreet (2021).

photon statistics and depends on the number of registered photons and the achieved S/N.

Each two successive exposures with orthogonal orientations of the QWP provide one circular polarisation measurement. The uncertainty of circular polarisation is the inverse of the S/N of the flux measured on both beams accumulated over all exposures. For a general formulation, see for example Patat & Romaniello (2006). For targets in the magnitude range $15 < V < 17$, typically 20−40 s individual exposure times were used. The delay between the exposures due to camera readout and QWP rotation is <0.3 s and is therefore negligible. In a typical nightly monitoring interval of 0.5−1.5 h, the number of individual measurements for one object is in the range 32−96. These data provide reliable statistical error estimates.

2.2. Target selection

Our target list comprises some WDs that are well studied in circular polarisation, and some WDs that have never been observed before. Well-studied targets include (1) WDs for which highly sensitive spectropolarimetric measurements failed to detect any magnetic field, and which may therefore be considered as non-magnetic standard WDs, (2) WDs that have relatively weak fields (from hundreds to several thousand kG), and (3) WDs that are known to exhibit a signal of BBCP. In addition to this group of 11 stars, we observed 5 DC WDs that were never observed before or in which we wished to confirm a previous detection. Our programme stars are listed in Table 1, together with a summary of each star's main features.

2.3. Data reduction

After the standard CCD image reductions (bias, dark), the fluxes of the o- and e-images were extracted with an aperture-optimising photometric algorithm that minimises the standard error of the mean value of the circular polarisation calculated from the individual measurements. The difference between the o- and e-beam intensities at the orthogonal orientations of the QWP (Sect. 2.1) yield one measurement of the Stokes parameter V/I, which is usually described as the net percentage circular polarisation. Depending on the seeing and star brightness, the optimum aperture radius was in the range 1.2″ to 2.8″, and the sky annulus radius was 1.5″ to 2.2″. To calculate the final value of V/I from individual measurements, we applied the 2σ weighting algorithm (Piirola et al. 2020), which gives a lower weight for points deviating by $>2\sigma$. Normally, 5−8% of the points deviated by more than 2σ and were given a weight $W < 1$. The remaining points (92−95%) were equally weighted ($W = 1$). The algorithm helps to suppress the effects of cosmic rays, transient clouds, or occasional moments of poor seeing.

3. Interpretation of the observed circular polarisation

It is important to realise that the presence of a magnetic field in a WD may lead to detectable broad-band circular polarisation through two quite different mechanisms. One mechanism is related to the continuum, and the other to the line opacity.

First, the spectrum of the star may include continuum radiation, outside even of the wings of possible discrete spectral features, which is circularly (and perhaps linearly) polarised. These polarised continua are expected to be produced by the subtle dependence of the sources of continuum opacity in the WD atmosphere on the magnetic field, so that the continuous opacity at a given wavelength is greater in one sense of circular polarisation than in the other, and the emergent continuum radiation has a net polarisation. The continuous opacity in cool H- or He-dominated WD atmospheres is due to combinations of opacity produced by free electrons, neutral atoms, negative atomic ions, and molecular ions. The result is that continuum polarisation is expected to depend on composition, $T_{\rm eff}$, and on the presence or absence of metallic impurities. A particularly simple treatment of this basic idea is described by Shipman (1971).

An example of the presence of true continuum polarisation is shown in Fig. 2 of Putney & Jordan (1995). In this figure, it is clear that in addition to the circular polarisation spikes coinciding with the σ components of Hα, there is a baseline of non-zero continuum circular polarisation, in spite of the absence of any absorption features other than the Zeeman triplet. This baseline

Table 2. Observing log of bright non-polarised standard stars.

Star	G	Date	UT	JD –	Exp.	V/I (%)		
		yyyy-mm-dd	hh:mm	2 400 000	(s)	B'	V'	R'
HD 115043	6.6	2021-07-02	21:19	59398.389	1280	-0.000 ± 0.001	-0.001 ± 0.001	-0.000 ± 0.001
HD 122676	6.9	2021-07-03	21:11	59399.383	1024	0.001 ± 0.001	0.001 ± 0.001	-0.000 ± 0.001
HD 124694	7.0	2021-07-04	21:19	59400.389	1152	-0.003 ± 0.001	-0.000 ± 0.001	0.001 ± 0.001
HD 211476	6.9	2021-07-03	05:00	59398.708	1600	0.002 ± 0.001	0.001 ± 0.001	-0.000 ± 0.001

continuum polarisation is produced by the continuous opacity effects mentioned above.

To provide a first estimate of magnetic field strength from detected non-zero continuum circular polarisation, we often make use of a simple order-of-magnitude estimate of the value of the line-of-sight average field $\langle B_z \rangle$ that causes the observed polarisation. This estimate assumes that the observed continuum value of V/I is very roughly proportional to $\langle B_z \rangle$, with a proportionality constant of about 15 MG per 1% circular polarisation. The origin of this estimate and derivation of the proportionality constant are discussed in detail by Bagnulo & Landstreet (2020) and references therein.

The resulting estimate of $\langle B_z \rangle$ can then be used to provide a (still less accurate) estimate, or at least a lower limit, of the mean surface field strength $\langle |B| \rangle$ by noting that $\langle |B| \rangle$ must be larger than its line-of-sight component ($\langle |B| \rangle > \langle B_z \rangle$), and we generally find $\langle |B| \rangle \geq 2.5 \langle B_z \rangle$ from experiments in which these two field strength values were computed for various dipolar and dipole-like magnetic field structures.

A second mechanism that leads to non-zero circular polarisation in broad-band filter measurements arises in MWDs that have strong polarised spectral features, such as polarised Zeeman splitting in the Balmer lines. Two examples are shown by Putney (1997) for GD 90 (with a field of $\langle |B| \rangle \approx 9$ MG) in her Fig. 1h and for PG 1658+441 (with a field of $\langle |B| \rangle \approx 2.3$ MG) in Fig. 1j. For both these stars, it is clear that the Zeeman pattern of Hα is practically symmetric, and so in a broad-band measurement, the two σ components will contribute approximately equal numbers of polarised photons, which because of the opposite signs of σ_+ and σ_- will lead (approximately) to no net polarised signal in the filter band.

However, at shorter wavelengths, it is no longer obvious that polarised counts contributed by the blue and red polarised signals from the σ components of each line will cancel: the quadratic Zeeman effect means that the spacing of various σ subcomponents is no longer the same in the blue and red features, and line saturation effects will change the equivalent widths of the polarised σ components so that they no longer cancel out in the filter measurement. In addition, the filter measurement may be made on a strongly sloped flux continuum, such as those seen in the intensity spectra of the two example stars, so that every blue-wing polarised feature will contribute more photons than the associated red-wing feature. For this reason also, the blue and red polarisation features will not exactly cancel, and the line spectrum will contribute to the net polarisation measured in a broad band that includes lines.

Thus we expect that polarisation in spectral line features may contribute some net circular polarisation to a broad filter measurement. We note, however, that while this effect means that a particular broad-band measurement may not provide an accurate measurement of the continuum polarisation between spectral lines, the line circular polarisation source still requires the presence of a magnetic field to operate. A broad-band filter measurement of a non-magnetic WD should yield a measurement without significant polarisation, and the detection of a broad-band circular polarisation signal is still a strongly valid sign of the presence of a magnetic field.

4. Results

Instrumental polarisation was determined from observations of four bright nearby stars, assumed to have zero circular polarisation (Sect. 4.1 and Table 2). The results of our WD observations are given in Table 3 and are presented in Sects. 4.2–4.5.

4.1. Observations of non-polarised bright stars

The high S/N measurements of non-polarised stars yield the instrumental polarisation to a precision better than 10^{-5}. In the $B'V'R'$ bands, the values of V/I are $0.0117 \pm 0.0006\%$, $0.0129 \pm 0.0005\%$, and $0.0084 \pm 0.0004\%$, respectively. The instrumental polarisation was subtracted from the observed polarisation of all targets, including the measurements of the standard stars in Table 2. The WDs in which non-zero circular polarisation was detected by our measurements are highlighted in boldface type in Table 3.

4.2. Known magnetic WDs with continuum polarisation

WD 1748+708 and WD 1900+705 are well-known high-field MWDs that exhibit strongly polarised continua. The polarisation of WD 1748+708 changes rapidly with λ (Angel et al. 1974). In Fig. 2 we compare our filter observations with an unpublished V/I spectrum of WD 1748+708 obtained by Angel and Landstreet on 1974 September 6.27 UT, using the Oke Multi-Channel Spectrophotometer on the Mount Palomar 5 m telescope, as described for example by Landstreet & Angel (1975). We note that the sign of V/I reverses within the V' passband. Polarisation values observed in adjacent passbands can be significantly different with broad-band filters. Accordingly, it is essential to make observations in more than one passband to search efficiently for magnetic WDs.

The spectropolarimetric data shown in the lower panel of Fig. 2 were obtained with the ISIS instrument on the *William Herschel* Telescope (WHT). The plotted data are adapted from the detailed search for possible variability of WD 1900+705 reported by Bagnulo & Landstreet (2019). We note that the broad $B'V'R'$ filters faithfully follow the broad outlines of the higher-resolution V/I spectra in both stars, clearly revealing the power of filter polarimetry even for complex polarised spectra.

4.3. Non-magnetic WDs

Stars WD 1647+591, WD 2032+248, and WD 2117+539 have previously been observed with highly sensitive spectropolarimetric techniques. All were found to be non-magnetic with

Table 3. Observing log of WDs. WD 1900+705 and WD 1831+197 were observed twice.

Star	Date	UT	JD –	Exp.	V/I (%)		
	yyyy-mm-dd	hh:mm	2 400 000	(s)	B'	V'	R'
WD 1647+591	2021-07-03	00:59	59398.541	1920	−0.000 ± 0.005	0.007 ± 0.007	0.004 ± 0.006
WD 2032+248	2021-07-04	05:00	59399.709	1920	0.001 ± 0.004	−0.001 ± 0.004	−0.002 ± 0.005
WD 2117+539	2021-07-03	04:17	59398.678	1800	0.000 ± 0.006	−0.001 ± 0.007	−0.007 ± 0.008
WD 1748+708	2021-07-03	00:10	59398.508	1920	0.665 ± 0.019	−0.376 ± 0.017	−1.126 ± 0.014
WD 1900+705	2021-07-02	22:22	59398.432	640	3.756 ± 0.016	3.604 ± 0.016	3.827 ± 0.019
WD 1309+853	2021-07-02	23:10	59398.466	3120	0.090 ± 0.048	0.109 ± 0.048	0.113 ± 0.037
WD 1350−090	2021-07-03	22:03	59399.419	2240	0.048 ± 0.015	0.017 ± 0.020	0.011 ± 0.018
WD 1503−070	2021-07-03	23:17	59399.471	3360	0.006 ± 0.030	0.042 ± 0.033	0.061 ± 0.025
WD 1953−011	2021-07-03	01:48	59398.576	2240	0.017 ± 0.012	0.015 ± 0.011	−0.012 ± 0.014
	2021-07-04	01:55	59399.580	3200	0.016 ± 0.007	0.002 ± 0.008	0.002 ± 0.008
WD 2254+076	2021-07-05	04:04	59400.671	5760	−0.347 ± 0.034	−0.324 ± 0.056	−0.529 ± 0.055
WD 1556+044	2021-07-04	22:10	59400.424	3200	−0.218 ± 0.033	0.315 ± 0.039	−0.131 ± 0.030
WD 1831+197	2021-07-04	00:37	59399.526	3840	−0.003 ± 0.038	0.049 ± 0.042	0.087 ± 0.037
	2021-07-04	23:48	59400.493	6400	0.051 ± 0.025	−0.015 ± 0.034	−0.089 ± 0.029
WD 1856+534	2021-07-05	01:33	59400.565	3840	−0.067 ± 0.058	−0.005 ± 0.060	−0.032 ± 0.043
WD 2011+063	2021-07-03	02:48	59398.618	3120	0.022 ± 0.035	0.057 ± 0.040	−0.028 ± 0.024
WD 2049-253	2021-07-04	03:31	59399.647	6400	0.442 ± 0.044	0.460 ± 0.039	0.684 ± 0.031
WD 2049-222	2021-07-05	02:39	59400.611	2240	0.095 ± 0.019	0.068 ± 0.022	0.142 ± 0.020

sub-kG accuracy through the analysis of the Zeeman effect on the Stokes V profiles of their very strong H Balmer lines. All these stars were observed by Bagnulo & Landstreet (2018) with the ISIS instrument of the WHT. ISIS has the capability of measuring polarisation in the continuum, but it has been found that the precision of these measurements is limited by the difficulty of correcting precisely for spurious background polarisation, particularly in measurements made in the presence of scattered moonlight, as discussed in detail by Bagnulo & Landstreet (2020). This effect means that it can be difficult to establish the reality of continuum polarisation detected with spectropolarimetry below about the 0.05% level. It is therefore very interesting to compare the very weak continuum polarisation signal observed with ISIS in these three non-magnetic WDs with the results of our new BBCP measurements. This comparison is shown in Fig. 3. The figure shows that for all non-magnetic WDs from the sample, DiPol-UF has measured zero continuum polarisation (<0.01%) in all three passbands. This null result strongly confirms that our BBCP measurements are free of any systematic or calibration errors at the level of $<10^{-4}$, and it also confirms the earlier conclusion about the serious difficulty of measuring continuum polarisation below about 0.05% with a spectropolarimeter, especially in the presence of moonlit background.

4.4. Weakly magnetic WDs

Our target list included five WDs that have been discovered to be magnetic from the Zeeman splitting of their spectral lines. In increasing order of field strength, these stars are WD 1350−090 and WD 1953−011, both with $\langle B_z\rangle \simeq 0.15$ MG; WD 1503−070, with $\langle|B|\rangle \sim 2$ MG; WD 1309+853, with $\langle|B|\rangle \sim 5.4$ MG; and WD 2254+076, with $\langle|B|\rangle \sim 16$ MG. These MWDs have been included in the study in order to clarify the relation between known magnetic field properties and observed continuum circular polarisation.

The only star in our sample of weakly magnetic WDs in which we firmly detect a signal of circular polarisation is WD 2254+076, although marginal detections are obtained in WD 1309+853 and WD 1350−090. As WD 2254+076 has the highest $\langle|B|\rangle$ value of the sample of low-field MWDs, this is not surprising. The other more weakly magnetic stars in this sample probe the limits of our ability to identify weakly magnetic WDs.

WD 2254+076 was discovered to host a magnetic field based on a flux spectrum from the Sloan Digital Sky Survey (SDSS) showing Zeeman-split H Balmer lines. Külebi et al. (2009) estimated a field of $\langle|B|\rangle \sim 16$ MG. Assuming that the star has a mean longitudinal field between 0 and 10 MG, we would expect to measure $|V/I|$ up to ~0.7%. Earlier observations by Angel et al. (1981), who had measured a BBCP signal of −0.16±0.10%, failed to detect a magnetic field in this star, but our measurements (−0.53 ± 0.06% in R', −0.32 ± 0.06% in V', and −0.35 ± 0.03% in B') are consistent with our prediction and would serve to definitively identify this WD as magnetic if this were not already known.

WD 1309+853 = G 256–7 was discovered to be magnetic by Putney (1995). From the spectra shown in her Fig. 2, we have deduced $\langle|B|\rangle \approx 5.4$ MG, while Putney found 4.9 MG. The polarisation spectrum reveals a non-zero $\langle B_z\rangle$. From the observations of Putney (1995), we can estimate $\langle B_z\rangle \sim 1-3$ MG. In this star, we have measured 0.113 ± 0.037 in the R' filter; in the B' and V' filter we have measured similar values of the polarisation, but only at ~2σ significance level. Because all the Balmer lines in this very cool DA star are extremely weak, all three filter measurements are probably dominated by continuum polarisation, which appears to be roughly constant with wavelength, as is found for the well-known similar DA star WD 0553–053 = G 99–47 (Angel & Landstreet 1972; Liebert et al. 1975). Both results are broadly consistent with the estimate that a field for which $\langle B_z\rangle = 15$ MG produces approximately 1% of circular polarisation in the continuum (Bagnulo & Landstreet 2020, and references therein), although more and better calibrations

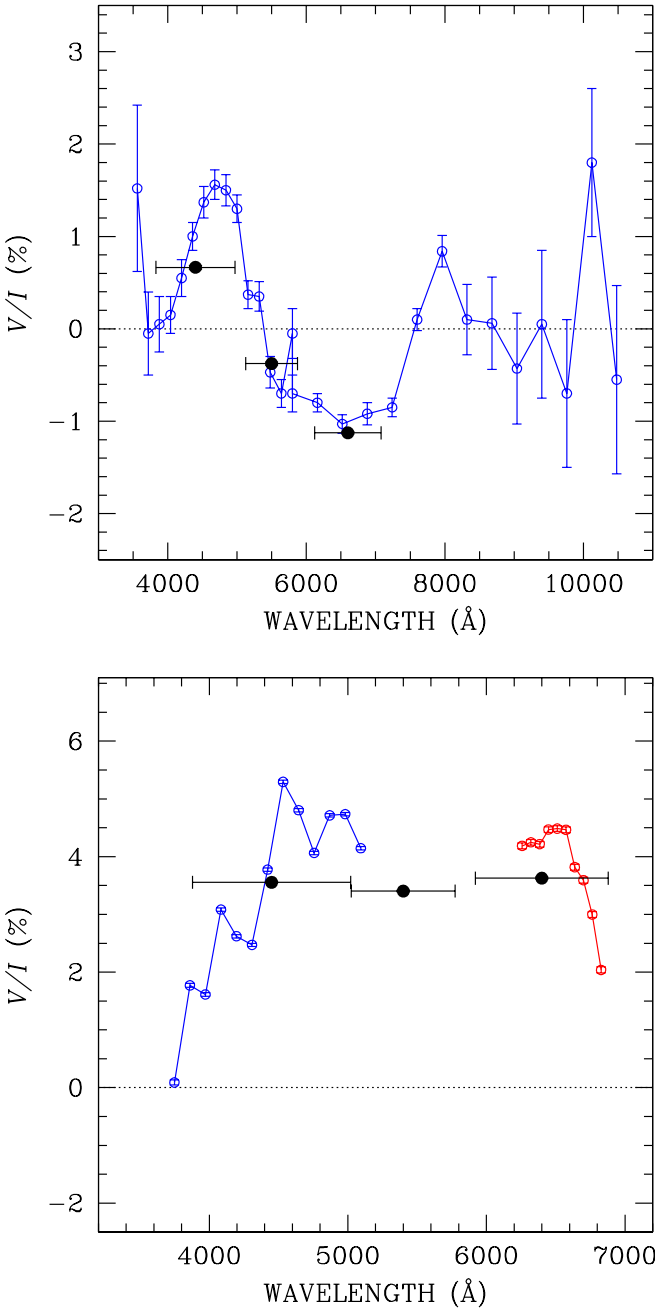

Fig. 2. V/I spectropolarimetry of the continuum (empty symbols joined by solid lines), and new DIPol-UF BBCP (solid circles) of the stars WD 1748+708 (*top panel*) and WD 1900+705 (*bottom panel*). Horizontal error bars represent the FWHM of the broad-band filters. The polarisation spectra used for comparison are described in the text.

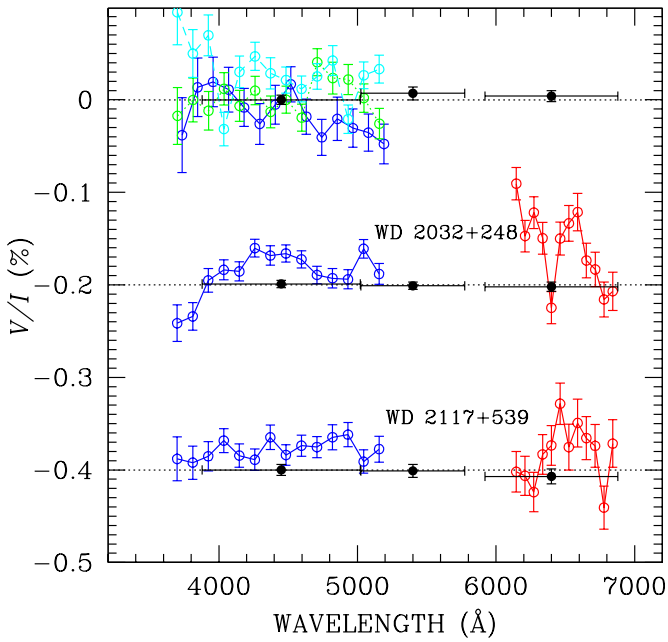

Fig. 3. ISIS spectropolarimetry of the continuum rebinned to 112 Å in the blue and 63 Å in the red (empty symbols joined by solid lines), and new DIPol-UF BBCP (solid circles) of three non-magnetic WDs. Star WD 1647+591 was observed three times with grating R600B, and observations obtained in different epochs are shown with different colours. The other two stars were observed simultaneously with gratings R600B and R1200R; see Bagnulo & Landstreet (2018) for more details. Data for different stars have been offset by 0, −0.2, and −0.4% for display purposes. Our BBCP measurements (zero polarisation) are consistent with no detectable magnetic field.

are needed to confirm the precision and range of usefulness of this approximation.

A field characterised by $\langle|B|\rangle \sim 2$ MG was discovered in WD 1503−070 by Gianninas et al. (2011) from Zeeman splitting of the shallow and weak Balmer lines. Our measurements set an upper limit of about 0.05% for circular polarisation. From the estimated $\langle|B|\rangle$ value, we would expect $|\langle B_z\rangle| \lesssim 1$ MG, that is, a signal of circular polarisation ≲0.07%. This estimate is consistent with our measurements.

In the star WD 1350−090, Schmidt & Smith (1995) measured $\langle B_z\rangle = 85 \pm 9$ kG. Bagnulo & Landstreet (unpublished) have measured the value of $\langle B_z\rangle$ several times, always with values between +105 and +145 kG, and Bagnulo & Landstreet (2021) have suggested that this field is actually roughly constant with time. We measured $V/I = 0.048 \pm 0.015\%$ in the B' filter, but found values lower than 0.02% in the other filters. For such a small $\langle B_z\rangle$ value, we would expect a signal of circular polarisation ≲0.01%.

However, this DA star has strong Balmer lines up to about H8 (where the higher lines merge), and has correspondingly strong line polarisation features throughout the B' filter. Thus we expect that the polarisation features across individual lines may well have failed to cancel exactly, either because of saturation effects, and/or because of the systematically biased weighting given by the continuum slope. Therefore we could reasonably expect some net polarisation precisely in the filter band that contains five Balmer lines, but not in the other two filter bands. In addition, the sharp cutoff of the B' filter is located in the blue wing of H8, and therefore the measurement did not give full weight to the blue σ polarisation from this line to cancel the polarised photons from the red σ component. Thus the polarisation detected in this band is almost certainly not a measurement of true continuum polarisation, but is a reliable symptom of the presence of magnetic field in this WD. In contrast, the null polarisation measurements in V' and R' are consistent with the prediction of continuum polarisation weaker than about 0.01%.

WD 1953−011 has a constant longitudinal field ≲0.1 MG (Valyavin et al. 2008) and should produce a BBCP signal also ≲0.01%. Our measurements, which failed to detect circular polarisation, rule out a signal significantly stronger than this value.

4.5. Science targets

We have firmly detected a signal of circular polarisation in three further WDs: WD 2049−253, WD 2049−222, and WD 1556+044. The DC star WD 2049−253 was discovered to be magnetic by Bagnulo & Landstreet (2020), who measured $V/I \simeq +0.5\%$, approximately constant between 370 and 510 nm, with the FORS2 instrument in spectropolarimetric mode. The flux spectrum of the star shows no obvious spectral line features, but with an effective temperature slightly below 5000 K, it could have an atmospheric chemistry dominated by either H or He. Although the spectropolarimetric measurement showed no obvious problems and was obtained during dark time so that polarised sky background due to cross-talk from highly polarised scattered moonlight was not a problem, the first measurement is near the limit of what can reliably be obtained with FORS. Bagnulo & Landstreet (2020) warned that the discovery needed to be confirmed by further observations. Our new detection of a signal at a similar level to that measured by Bagnulo & Landstreet (2020) fully confirms that the star is indeed magnetic, with a field that is, as estimated by Bagnulo & Landstreet (2020), probably characterised by $\langle B_z \rangle \sim 7$ MG and so by $\langle |B| \rangle$ of about 20 MG or slightly higher.

WD 1556+044 and WD 2049−222 are DC WDs that have never been observed in polarimetric mode. They represent the first discovery of new MWDs obtained by means of BBCP since the discoveries in the 1970s that were summarised by Angel et al. (1981).

WD 2049−222 was first identified as a DC star in the survey of hot stars in the Galactic halo of Bergeron et al. (1992). This classification was confirmed by Kawka & Vennes (2006), who showed a portion of the spectrum between 6340 and 6780 Å. The completely smooth spectrum segment supports the classification of this WD as a DC. There is a significant spread in the values of $T_{\rm eff}$ that are found by different investigators, but they generally range between 8000 and 9500 K. The absence of the slightest indication of Hα in the spectrum segment published by Kawka & Vennes (2006) at this effective temperature means that the dominant atmospheric chemistry is very probably He. The polarisation signal that we have measured in WD 2049−222 is possibly the weakest non-zero polarisation signal ever detected in a WD. It is weaker than that measured in WD 0553+053 = G99–47 by Angel & Landstreet (1972), which is −0.4% at 4000 Å and −0.2% at 8000 Å, and even weaker than that observed in WD 1116−470 by Bagnulo & Landstreet (2021), which was just ≃−0.2% in the entire range from 4000 to 9000 Å, but which in fact still awaits confirmation.

The broadband polarisation measurements of WD 2049–222 all have the same sign, but the variations appear to be real, with the maximum signal $V/I = 0.142 \pm 0.020\%$ found in the R' band. For this star, we estimate $\langle B_z \rangle = 1-2$ MG. The fact that the polarisation in all three broad bands has the same sign is typical of the polarisation spectra of most MWDs showing non-zero continuum circular polarisation, from WDs with very strong continuum polarisation, such as WD 1900+705 to the weak continuum polarisation of WD 0553+053. In this star, the available evidence suggests that the observed polarisation is probably true continuum polarisation.

WD 1556+044 was originally thought to be a quasi-stellar object (Véron-Cetty & Véron 2010), but was recognised as a DC WD by Limoges et al. (2013), who showed its blue I spectrum to about 5200 Å. The spectrum is apparently completely featureless even at high S/N, and with $T_{\rm eff} = 6685$ K, the star very probably has an He-rich atmosphere. Like many MWDs, the mass of this WD, 0.85 $M_\odot$, is considerably higher than those of most of the stars in Table 1. The polarisation in WD 1556+044 is detected at the 6σ, 8σ, and 4σ levels in the B', V', and R' filters. In this new MWD, the detection is quite firm, and the polarisation values, which change sign from B' to V' to R', indicate strong variations of V/I with wavelength. This is an unusual characteristic that is found in only a small minority of MWDs for which the spectrum of V/I is well established. This unusual characteristic is perhaps most similar to the variation seen in WD 1748+708 = G240–72 (Fig. 2), which is only about 1000 K cooler. The explanation for the unusual sign changes in these two MWDs is unknown, but may involve similar chemical pollution of the nearly pure He atmospheres. This new MWD could have a magnetic field of $\langle B_z \rangle \sim 5$ MG, and a field $\langle |B| \rangle$ that is at least 12 or 15 MG, and perhaps larger.

We now comment on the remaining three science targets, for which we are able to set only upper limits for $|V/I|$ and $|\langle B_z \rangle|$. Among these targets, WD 1856+534 is of special interest because Vanderburg et al. (2020) discovered a giant planet orbiting it that has not been tidally disrupted. The star has never been observed in polarimetric mode, and our measurements suggest that the star's circular polarisation is most likely <0.1% (in absolute value), setting our estimate of the upper limit for $|\langle B_z \rangle|$ to 1 MG.

We observed WD 1831+197 twice. With our first observation, we obtained a detection of nearly 3σ with the R' filter. Taken at a face value, our second observation represents a 3σ detection (but with the opposite sign with respect to the previous night). Owing to the lack of detection in the other filters, we cannot yet accept the star as a MWD, but it would be worthwhile to re-observe it with a larger telescope, or with a much longer exposure time. The star could have a field of about 1 MG and might be variable. At the same time, our observations probably rule out the presence of a field with a longitudinal component larger than a few MG.

WD 2011+063 was one of the first WDs ever observed in polarimetric mode: Angel & Landstreet (1970b) measured $V/I = 0.12 \pm 0.09\%$. Our new measurements are about three times more accurate, but still detect no polarisation signal. The upper limit for $|\langle B_z \rangle|$ is again of about 1 MG.

5. Polarimetric sensitivity and detection limits

Our observing run may be used to make quantitative predictions regarding the level of polarimetric sensitivity that may be achieved for the BBCP measurements as a function of time, stellar magnitude, and telescope size using DIPol-UF with our filter set. Figure 4 shows our measurement uncertainties in the $B'V'R'$ filters, normalised to 1 h exposure time, as a function of the *Gaia* magnitude G. Uncertainties depend on the spectral energy distribution of the star, that is, for hot stars, the increased flux in the blue reduces errors in the B' band, whereas for cool stars, the best S/N is achieved in the red. For our sample of stars and their spectral energy dependence, the errors are rather uniformly distributed (Fig. 4). The high throughput of the B' band (Fig. 1) helps to balance the performance of the DIPol-UF instrument in the different passbands recorded simultaneously.

The relationship obtained for the polarimetric uncertainty as a function of the input flux indicates that the former is defined by the photon flux with no detectable systematic errors (both axes in Fig. 4 are logarithmic). This nicely demonstrates that the DIPol-UF polarimeter provides polarimetric measurements with precision and accuracy down to 10 parts per million (ppm) also in circular polarisation, that is, it is comparable to the few

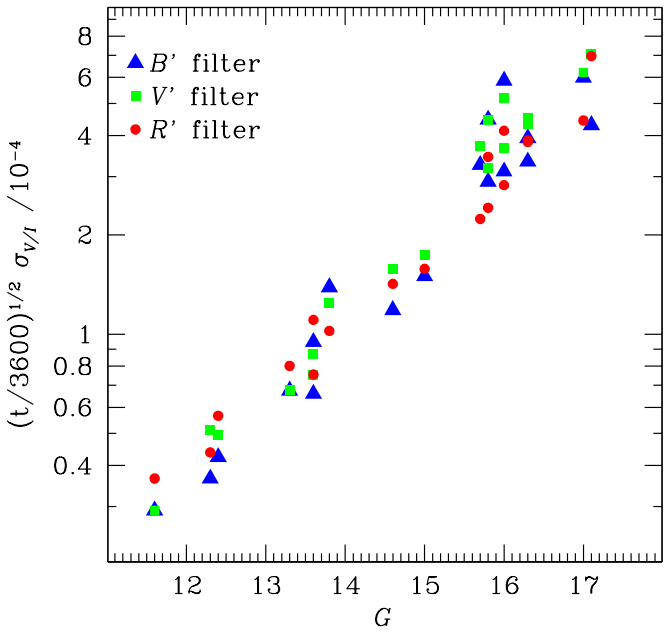

Fig. 4. Relation between magnitude and uncertainty of our measurements of Table 3 as a function of *Gaia G* magnitude, normalised to 1 h exposure time.

ppm uncertainty achieved in linear polarisation measurements (Piirola et al. 2021). Thus, using this relation, we can evaluate observational requirements for a given WD magnetic field with DIPol-UF employed at various telescopes.

From the estimate that a $\langle B_z \rangle = 15$ MG field produces a polarisation of approximately 1% in the continuum (Bagnulo & Landstreet 2020, and references therein), it follows that a signal of ~0.07% is expected from a $\langle B_z \rangle = 1$ MG field. A 3σ detection of this requires an uncertainty of ~0.02%. According to the relation in Fig. 4, this is achieved in one hour for a star with a magnitude of $G \sim 15.5$. For a brighter $G \sim 12$ star, the precision 0.004% in one hour would yield a 3σ detection of $\langle B_z \rangle \sim 0.2$ MG. For the faintest ($G \sim 17$) stars in our sample, the precision achieved in one hour would allow $>3\sigma$ detection of fields $\langle B_z \rangle > 3$ MG.

The typical seeing values (0.6″−1.0″) and the sky darkness during our observations are comparable to the conditions at the best observing sites, and our detection limits could easily be scaled to larger telescopes. For an 8 m telescope, the measured polarisation uncertainties would be lower by a factor of ~3 for a given exposure time.

6. Conclusions

During the past two years, five new MWDs of spectral class DC have been discovered: WD 0004+122, WD 078−670, WD 2049−253 (discoveries presented by Bagnulo & Landstreet 2020, with confirmation for the latter obtained in this work), WD 1556+044, and WD 2049−222 (this work), while the discovery of a ~20 MG field in WD 1116−47 by Bagnulo & Landstreet (2021) still needs to be confirmed. These are the first discoveries of magnetic fields in old, featureless WDs since the mid-1990s by Putney (1995). WD 1556+044 and WD 2049−222 represent the first discoveries obtained by means of BBCP filter measurements since the late 1970s. The significance is that we are now able to explore the magnetic features of stars in the last stages of stellar evolution. In particular, studying the frequency of the occurrence of magnetic fields in old WDs will allow us to understand if and when Ohmic decay acts during the long WD cooling phase, or if magnetic fields are found with high frequency and high field strength even among the very oldest WDs of our neighbourhood.

Acknowledgements. Based on observations made with the Nordic Optical Telescope, owned in collaboration by the University of Turku and Aarhus University, and operated jointly by Aarhus University, the University of Turku and the University of Oslo, representing Denmark, Finland and Norway, the University of Iceland and Stockholm University at the Observatorio del Roque de los Muchachos, La Palma, Spain, of the Instituto de Astrofisica de Canarias. DIPol-UF is a joint effort between University of Turku (Finland) and Leibniz Institute for Solar Physics (Germany). We acknowledge support from the Magnus Ehrnrooth foundation and ERC Advanced Grant Hot-Mol ERC-2011-AdG-291659. JDL acknowledges the financial support of the Natural Sciences and Engineering Research Council of Canada (NSERC), funding reference number 6377-2016.

References

Angel, J. R. P., & Landstreet, J. D. 1970a, ApJ, 160, L147
Angel, J. R. P., & Landstreet, J. D. 1970b, ApJ, 162, L61
Angel, J. R. P., & Landstreet, J. D. 1972, ApJ, 178, L21
Angel, J. R. P., Hintzen, P., Strittmatter, P. A., & Martin, P. G. 1974, ApJ, 190, L71
Angel, J. R. P., Borra, E. F., & Landstreet, J. D. 1981, ApJS, 45, 457
Aznar Cuadrado, R., Jordan, S., Napiwotzki, R., et al. 2004, A&A, 423, 1081
Bagnulo, S., & Landstreet, J. D. 2018, A&A, 618, A113
Bagnulo, S., & Landstreet, J. D. 2019, MNRAS, 486, 4655
Bagnulo, S., & Landstreet, J. D. 2020, A&A, 643, A134
Bagnulo, S., & Landstreet, J. D. 2021, MNRAS, 507, 5902
Berdyugin, A. V., & Piirola, V. 1999, A&A, 352, 619
Bergeron, P., Ruiz, M.-T., & Leggett, S. K. 1992, ApJ, 400, 315
Gianninas, A., Bergeron, P., & Ruiz, M. T. 2011, ApJ, 743, 138
Isern, J., Garsia-Berro, E., Kulebi, B., & Loren-Aguilar, P. 2017, ApJ, 836, L28
Kawka, A., & Vennes, S. 2006, ApJ, 643, 402
Kemp, J. C., Swedlund, J. B., Landstreet, J. D., & Angel, J. R. P. 1970, ApJ, 161, L77
Külebi, B., Jordan, S., Euchner, F., Gänsicke, B. T., & Hirsch, H. 2009, A&A, 506, 1341
Landstreet, J. D., & Angel, J. R. P. 1971, ApJ, 165, L67
Landstreet, J. D., & Angel, J. R. P. 1975, ApJ, 196, 819
Landstreet, J. D., & Bagnulo, S. 2019, A&A, 623, A46
Liebert, J., Angel, J. R. P., & Landstreet, J. D. 1975, ApJ, 202, L139
Liebert, J., & Stockman, H. S. 1980, PASP, 92, 657
Limoges, M. M., Lépine, S., & Bergeron, P. 2013, AJ, 145, 136
Patat, F., & Romaniello, M. 2006, PASP, 118, 146
Piirola, V., Berdyugin, A., & Berdyugina, S. 2014, in Ground-based and Airborne Instrumentation for Astronomy V, eds. S. K. Ramsay, I. S. McLean, & H. Takami, SPIE Conf. Ser., 9147, 91478I
Piirola, V., Berdyugin, A., Frisch, P. C., et al. 2020, A&A, 635, A46
Piirola, V., Kosenkov, I. A., Berdyugin, A. V., Berdyugina, S. V., & Poutanen, J. 2021, AJ, 161, 20
Putney, A. 1995, ApJ, 451, L67
Putney, A. 1997, ApJS, 112, 527
Putney, A., & Jordan, S. 1995, ApJ, 449, 863
Schmidt, G. D., & Smith, P. S. 1994, ApJ, 423, L63
Schmidt, G. D., & Smith, P. S. 1995, ApJ, 448, 305
Shipman, H. L. 1971, ApJ, 167, 165
Valyavin, G., Wade, G. A., Bagnulo, S., et al. 2008, ApJ, 683, 466
Vanderburg, A., Rappaport, S. A., Xu, S., et al. 2020, Nature, 585, 363
Véron-Cetty, M. P., & Véron, P. 2010, A&A, 518, A10
West, S. C. 1989, ApJ, 345, 511